1 Running title: Complete life cycle of the bioluminescent California Sea Firefly

2

3

4 **Laboratory culture of the California Sea Firefly *Vargula tsujii* (Ostracoda: Cypridinidae):**

5 **Developing a model system for the evolution of marine bioluminescence**

6

7 Jessica A. Goodheart[1], Geetanjali Minsky[1], Mira N. Brynjegard-Bialik[1], Michael S. Drummond[1], J. David

8 Munoz[2], Timothy R. Fallon[3,4], Darrin T. Schultz[5,6], Jing-Ke Weng[3,4], Elizabeth Torres[2] & Todd H.

9 Oakley*[1]

10

11 [1] Department of Ecology, Evolution, and Marine Biology, University of California, Santa Barbara, Santa

12 Barbara, CA 93106

13 [2] Department of Biological Sciences, California State University, Los Angeles, CA 90032-8201, USA

14 [3] Whitehead Institute for Biomedical Research, Cambridge, MA, 02142, USA

15 [4] Department of Biology, Massachusetts Institute of Technology, Cambridge, MA 02142, USA

16 [5] Monterey Bay Aquarium Research Institute, Moss Landing, CA 95060, USA

17 [6] Department of Biomolecular Engineering and Bioinformatics, University of California, Santa Cruz,

18 Santa Cruz, CA 96060, USA

19

20

21 *Corresponding author: oakley@lifesci.ucsb.edu

22

23

24

25

26

27 **Abstract**

28 Bioluminescence, or the production of light by living organisms via chemical reaction, is

29 widespread across Metazoa. Culturing bioluminescent organisms from diverse taxonomic

30 groups is important for determining the biosynthetic pathways of bioluminescent substrates,

31 which may lead to new tools for biotechnology and biomedicine. Although some previously

32 cultured luminescent groups represent independent origins of bioluminescence, cnidarians,

33 ctenophores, and brittle stars use luminescent substrates (luciferins) obtained from their diets,

34 and therefore are not informative for determination of the biosynthethic pathways of the

35 luciferins. Terrestrial fireflies do synthesize their own luciferin, but the biosynthetic pathway for

36 firefly luciferin remains unclear. An additional independent origin of endogenous

37 bioluminescence is found within ostracods from the family Cypridinidae, which use their

38 luminescence for defense and, in Caribbean species, for courtship displays. Here, we report the

39 first complete life cycle of a luminous ostracod (*Vargula tsujii*, the California Sea Firefly) in the

40 laboratory. We also describe the embryonic development of *Vargula tsujii* and discuss the size

41 classes of instar development. We find embryogenesis in *V. tsujii* ranges between 25-38 days,

42 and this species appears to have five instar stages, consistent with ontogeny in other cypridinid

43 lineages. We estimate a complete life cycle at 3-4 months. We present the first complete

44 mitochondrial genome for *Vargula tsujii*. Finally, we find no evidence of significant population

45 genetic structure or cryptic species throughout the southern California range of *V. tsujii*. Bringing

46 a luminous ostracod into laboratory culture sets the stage for many potential avenues of study,

47 including the biosynthetic pathway of cypridinid luciferin and genomic manipulation of an

48 autogenic bioluminescent system.

49

52

Introduction

The production of bioluminescence in animals is an important biological innovation that is particularly prevalent in marine environments [1]. To produce light, animals combine an enzyme (usually a luciferase or photoprotein) and a substrate (luciferin) with oxygen, and sometimes additional components such as ATP or calcium [2–4]. Although the enzymes that produce light are well-studied [5–13], and we know how the substrate is produced in bacteria [14] and fungi [15], we do not yet know how luciferin is synthesized in any animal system. A comprehensive understanding of this pathway could be transformative for optogenetics in transgenic organisms, where the ability to produce bioluminescence in situ as a biosensor or light source would be invaluable. Some laboratory-reared luminescent animals already exist (Table 1), but may not be suitable for studying luciferin biosynthesis. In particular, ctenophores, cnidarians, and brittle stars use coelenterazine obtained from their diet as a substrate [1]. Fireflies do use an endogenous luciferin specific to Coleoptera (beetles) [16], but they often have longer life cycles than other taxa, slowing research progress [17]. Although there are other independent origins of autogenic bioluminescence, which we define as that produced via luciferase and luciferin that are synthesized via the genome of the light producing animal, no laboratory cultures exist yet. This makes additional studies focused on the comparative evolution of this ability extremely challenging.

Ostracods from the family Cypridinidae independently evolved bioluminescence, and use a luciferin that is endogenous to ostracods and chemically different from that of other bioluminescent organisms [2,18,19]. Of the metazoan taxa already cultured, autogenic luminescence is only known to occur within fireflies [20,21]. Due to the independent origin of ostracod bioluminescence in the family Cypridinidae, and evidence for the autogenic nature of the necessary luciferin and luciferase, ostracods represent a critical lineage for understanding how bioluminescence evolved. Establishing laboratory cultures of luminescent ostracods within

3

79   Cypridinidae would pave the way for investigations into the biosynthetic pathway of luciferins in

80   Metazoa, as well as comparative studies of the biochemistry, physiology, genetics, and function

81   of endogenous bioluminescence.

82

83   Cypridinidae is estimated to include over 300 ostracod species [22], some of which use

84   bioluminescence for defense, while others possess the ability to create bioluminescent courtship

85   displays in addition to defensive secretions [23]. Lineages with sexually dimorphic bioluminescent

86   displays, such as those in Cypridinidae, have more species than their non-displaying sister

87   lineages, indicating that origins of bioluminescent courtship may increase diversification rates

88   (Ellis and Oakley 2016). As such, cypridinid ostracods represent an excellent system for

89   understanding how behavioral diversification can lead to increases in species accumulation.

90   Furthermore, cypridinid ostracods diversified while generating bioluminescence with a

91   consistent biochemical basis across the clade [24], meaning that they use the same luciferin and

92   homologous enzymes to make light. The conserved nature of the luminescent chemical reaction

93   provides a system within which bioluminescence can produce rapid changes in phenotypic

94   diversity by modifying amino acid sequences of the enzyme or how the enzyme is used [25].

95

96   Attempts to culture luminescent and non-luminescent species of Cypridinidae have led to

97   varying success, including *Skogsbergia lerneri* (non-luminous species with no mating in culture)

98   [26], *Photeros annecohenae* (luminous species without the complete life cycle in culture) [27], and

99   *Vargula hilgendorfii* (luminous species with no mating in culture) [28]. Researchers attempting to

100   culture *Vargula hilgendorfii* tried multiple alternative aquarium set-ups and tested sensitivity to

101   nutrients commonly measured in aquaria, but were still unable to induce mating in the lab [28]. An

102   unnamed species of luminescent ostracod is claimed to have been cultured at the CTAQUA

103   Foundation (Aquaculture and Technological Centre) in Spain for molecular gastronomy [29], but

104   no information on species, culture longevity, or whether mating occurred is available on this

105   enigmatic and uncertain culture. Other non-cypridinid ostracods have been reared in the

106   laboratory as well, including the myodocopids *Euphilomedes carcharodonta* [30] and

107   *Euphilomedes nipponica* [31] and the podocopid *Xestoleberis hanaii* (only record of copulation in

108   the laboratory for any ostracod) [32].

109

110   In this paper, we present evidence that we are the first to rear a luminous ostracod (*Vargula*

111   *tsujii*) through its complete life cycle in the laboratory. *Vargula tsujii* is the only bioluminescent

112   cypridinid ostracod described from the Pacific coast of North America. Commonly found in

113   southern California, the reported range of *V. tsujii* is from Baja California to Monterey Bay [33].

114   This species is primarily active in the kelp canopy at night [34]. Similarly to some other cypridinid

115   ostracods, *Vargula tsujii* is a scavenger, and is presumed to feed on dead and decaying fish and

116   invertebrates on the benthos since it can be collected via baited traps. However, some authors

117   also observed *V. tsujii* attacking the soft tissues of live fishes caged nearshore [35]. *Vargula tsujii*

118   is an important prey item of the plainfin midshipman fish (*Porichthys notatus*), as it is the source

119   of luciferin for the bioluminescence seen in the fish [36].

120

121   In addition to evidence for the completion of the life cycle of *Vargula tsujii* in the laboratory, we

122   provide a successful methodology for culturing individuals of *V. tsujii*, descriptions and analyses

123   of embryogenesis and instar development, a reconstruction of its mitochondrial genome, and a

124   brief description of the distribution of molecular diversity of *V. tsujii* across coastal southern

125   California.

126

127

128   **Methods**

129   *Specimen collection*

5

130   We collected *Vargula tsujii* from three primary locations: (1) Fisherman's Cove near Two

131   Harbors on Catalina Island, CA, USA (33°26'42.5"N 118°29'04.2"W) directly adjacent to the

132   Wrigley Marine Science Center, (2) Cabrillo Marina, Los Angeles, CA, USA (33°43'13.5"N

133   118°16'47.4"W), and (3) Shelter Island public boat ramp, San Diego, CA, USA (32°42'56.3"N

134   117°13'22.9"W) (Figure 1; Table 2). We also provide locations in Figure 1 and Table 2 where we

135   set traps but did not collect *V. tsujii*. The specimens used for culture and description of the life

136   cycle of *V. tsujii* were exclusively from Fisherman's Cove, Catalina Island, and we collected

137   additional specimens from the Cabrillo Marina and Shelter Island public boat ramp to discern

138   the genetic diversity of *V. tsujii* and test for the presence of any cryptic species. For specimen

139   collection we used Morin pipe traps: cylindrical polyvinyl chloride (PVC) tubes with mesh funnels

140   to prevent the ostracods from escaping once they entered [37]. We baited traps with dead fish or

141   fresh chicken liver (roughly 1-2 cm^3). We set traps in 1-10 meters of water at sunset and

142   collected them 1.5 to 2 hours after last light to allow time for the ostracods to accumulate.
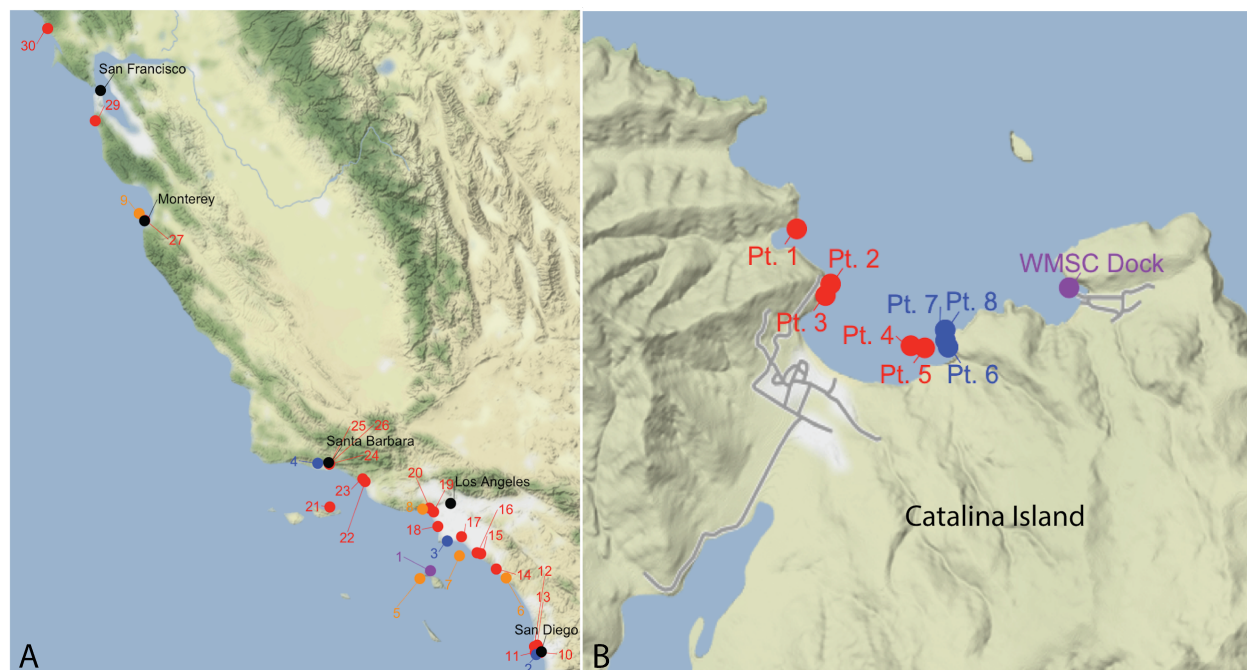

143

Figure 1. Map of localities where collections (and attempted collections of Vargula tsujii were made). Black points represent geographic annotations for reference, purple points refer to the location where ostracods were collected that were ultimately cultured, blue where animals were found or collected, orange where Kornicker originally collected animals, and red where no V. tsujii were found. (A) Map of the California (USA) coastline where V. tsujii collections were attempted; (B) Map of the region near Two Harbors (Santa Catalina Island, California, USA) where V. tsujii collections were attempted.

144

145

6

146   *Population genetic analyses*

147   We obtained *Vargula tsujii* sequence data for 16S rRNA (16S) and cytochrome oxidase 1 (COI)

148   from a previously published thesis [38]. We then aligned and visually inspected sequence

149   chromatograms with Sequencer version 3.1 (Gene Codes Corp) (Table S1). We constructed

150   haplotype networks for the two genes, COI (Number of individuals: Catalina, 18; San Diego, 11;

151   San Pedro, 12) and 16S (Number of individuals: Catalina, 19; San Diego, 20; San Pedro, 21)

152   (Figure 3) with the package pegas [39] in the R environment (version 3.4.2) [40]. To assess whether

153   sequences within populations cluster together, we analyzed each gene via Discriminant

154   Analysis of Principal Components (DAPC) using the adegenet package in R [41] and compared

155   models with one, two, and three clusters using the Bayesian Information Criterion (BIC) [42].

156

157   *Description of aquarium system and feeding*

158   We cultured *Vargula tsujii* at the University of California, Santa Barbara in aquariums designed

159   for water to flow through sand and out the bottom. This allowed continuous water flow to keep

160   water fresh, and not suck ostracods into a filter. Instead, ostracods remain in sand where they

161   spend the daylight hours. We kept animals under a 12:12 light cycle with an indirect blue LED

162   light.

163

164   We first modified a five gallon glass tank by drilling a hole in the bottom, which was then

165   covered with the bottom of an undergravel filter and a 3 cm layer of commercial aragonite sand

166   for aquariums. To maintain continuous water flow, we used plastic tubing (diameter = 1 cm)

167   connected directly to an overflowing reservoir tank, which created a siphon system for moving

168   water into the tank (Figure 2). The siphon provided continuous water flow when needed, and

169   prevented overflow of the aquarium. In addition, to prevent a complete drain of the water if the

170   siphon flow broke, which is common with larger siphons, we attached an outflow pipe to the

171   bottom of the aquarium that drained halfway up the side of the tank (Figure 2).

172

173   We also created a similar system for smaller experimental aquaria, though these appeared to

174   be less effective long-term, as we saw high mortality in non-systematic studies. For the small

175   aquaria ("condos"), we cut a large hole (~5 cm diameter) into the bottom of seven 500 mL

176   Nalgene™ Square PETG Media Bottles with Septum Closures (Figure 2F). We then modified a

177   100 μm cell strainer to fit in the bore of the media bottle in such a way that it would remain there

178   when the closure of the media bottle was screwed back on, allowing water but not sand to flow

179   through. We inverted the bottle and added a ~3 cm layer of sand to the bottom, above the cell

180   strainer, measured from the edge of the bottle cap. For these smaller aquaria, we used 5 mm

181   diameter tubing as siphons from the reservoir tank and for the outflow. Similar to the large tank,

182   the outflow tubes (placed in the septum closure) drained roughly halfway up the side of the

183   aquaria to prevent the water from draining completely.

184

185   Most recently, we created custom aquariums from acrylic (Fig. 2G), with similar dimensions to

186   the 5-gallon glass aquarium. We installed a bulkhead in the bottom and attached PVC tubing as

187   a drain, which we again raised to about half the height of the aquarium to prevent complete

188   drainage if inflow of water stops accidentally. We added a valve to control the rate of outflow

189   and instead of a siphon, we added a float switch to set inflow rate.
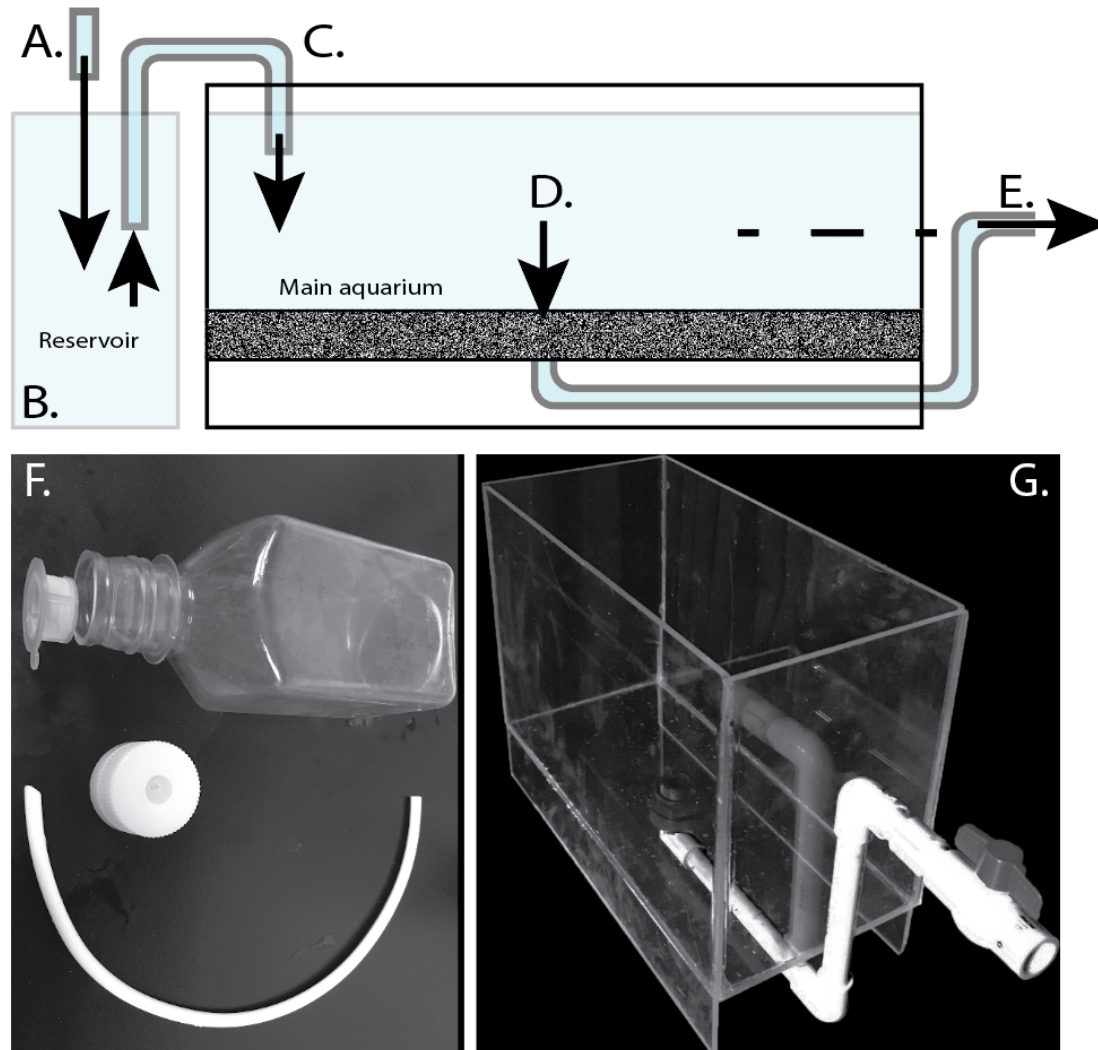
190

191

Figure 2. Diagrammatic representation of aquarium setup for sea fireflies. (A) Source water flows into (B) a reservoir tank, which overflows to keep the reservoir full and water level constant. (C) We use a siphon to carry water from a reservoir tank to main aquarium where ostracods live. Water level of the main tank drains through sand (stippled), through (E) an outflow that is raised to a level that would cause water to remain at the level of the dashed line, even if a siphon is interrupted to cause water to stop flowing into the main tank. (F) Plastic bottle and parts used to create small aquarium using the same logic as main aquarium. (G) Custom-built acrylic aquarium with drain in bottom and raised outflow with adjustable rate.

We initially offered the ostracods multiple diet choices, including: (1) imitation crab, which is primarily pollock, (2) carnivore fish pellets or fish flakes, (3) tilapia fillets, and (4) anchovies, which have each made for successful food sources in Caribbean ostracods (Todd Oakley, personal observation; [27,37]). Although the adults appeared moderately interested in these food sources in non-systematic trials, we found the juvenile ostracods did not eat them, but they did

202   actively feed on raw chicken liver, as do *Vargula hilgendorfii* individuals from Japan [43]. In

203   culture, we therefore provided pieces of chicken liver daily (~1 cm^3 per 200 animals). Due to the

204   nocturnal life history of *V. tsujii*, we fed them in the late afternoon or early evening (around the

205   beginning of the dark cycle), and removed the food from the aquarium in the morning (~3-5

206   hours into the light cycle) to reduce the chance of bacterial fouling.

207

208   *Rearing of embryos*

209   We tested two primary methods for rearing embryos. The first was less successful in terms of

210   longevity of both the mothers and embryos, but provided usable data on embryogenesis.

211   Regardless of rearing method, ostracods did not appear to eat while they were brooding.

212

213   For the first method, we kept females individually in circular wells in twelve-well dishes [27], with

214   approximately 1 mL of 17°C seawater. We recorded visual observations of the females and their

215   embryos and changed the water daily. The advantage of this method is ease of identification

216   and observation of individual ostracods, allowing us to track the growth of specific embryos over

217   a given period of time. However, all females which deposited embryos into the brooding

218   chamber died before their embryos were released from the marsupium, although the precise

219   cause of death is unknown. These embryos were then removed from the female marsupium by

220   dissection, kept in wells, and observed until the animals hatched through the chorion (see

221   Supplemental Video).

222

223   For the second method, we identified and removed brooding females from the aquarium and

224   placed them in 50 mL Falcon™ tubes (2 females per tube). Roughly 5 mL of sand was added to

225   the bottom of each tube to allow females to burrow. Falcon tubes were then placed in a large

226   seawater reservoir that ranged from 17-19°C. We changed the water in each tube daily, and

227   imaged brooding females every other day with a camera attached to a dissecting scope. We

228   used key diagnostic features such as number of embryos and female size to distinguish

229   individual females from one another. Of the thirteen individuals kept in Falcon^TM tubes, only one

230   died prior to embryo release from the marsupium.

231

232   *Animal measurements and determination of instar size classes*

233   We imaged ostracods across all life stages using a standard dissecting microscope and an

234   Olympus brand camera, and measured the carapace length, carapace height, eye width, and

235   keel width with the software Fiji (Sample size = 626 individuals; Table S3)[44]. These parameters

236   are useful in the determination of the instar stages in other bioluminescent ostracods [27]. A

237   subset of these individuals (9 males, 11 females) were dissected to confirm sex. We partitioned

238   the data into clusters using the KMeans clustering algorithm implemented in scikit-learn [45] in

239   Python 2.7 [46]. KMeans fits the data into k clusters, specified in the arguments, sorting each data

240   point into the cluster which has the minimum euclidean distance to the centroid of the cluster.

241   The value for k was originally specified as eight based on the five known stages of instar

242   development for related species of ostracods plus the embryonic stage and adult males and

243   females. However, a k-value of eight clusters resulted in a split of the inferred adult female

244   cluster into two clusters rather than the discrimination of adult males from inferred A-I instars. To

245   avoid this apparent over-clustering, we ran our final analysis with a k-value of seven, which

246   retained all inferred adult females in a single cluster but was unable to distinguish an adult male

247   cluster from the inferred A-I instars. We assigned development stages to each cluster based on

248   the relationship by comparison to the closely related *Photeros annecohenae*, which grew in 12-

249   well dishes to allow more precise documentation of instars [27].

250

251   *Whole genome sequencing*

11

252   We froze four adult female *Vargula tsujii*, collected from the WMSC Dock on 2017-09-01 in

253   liquid nitrogen and shipped the specimens on dry-ice to the Hudson Alpha Institute for

254   Biotechnology Genomic Services Lab (HAIB-GSL) for genomic DNA extraction and Chromium

255   v2 Illumina sequencing library preparation. HAIB-GSL extracted the DNA using the Qiagen

256   MagAttract Kit, yielding 141 ng, 99 ng ,153 ng , and 96 ng of extracted DNA respectively. This

257   quantity of DNA was not sufficient for a size distribution analysis via agarose pulse field gel

258   analysis, therefore we decided to proceed with Chromium v2 library prep with the 153 ng

259   sample (sample # 5047), without confirmation of a suitable high-molecular weight DNA size

260   distribution. We sequenced this library on three lanes of a HiSeqX instrument using a 151x151

261   paired-end sequencing mode, resulting in a total of 910,926,987 paired reads (260.6 Gbp). We

262   attempted whole genome assembly of the resulting sequencing data with the Supernova v2.0.0

263   genome assembly software [47]. We then used the Agilent Femto Pulse High Molecular Weight

264   DNA capillary electrophoresis instrument at the MIT BioMicro Center to perform a post

265   sequencing analysis of the size distribution of the DNA used for Chromium library preparation.

266

267   *Mitochondrial genome assembly*

268   To achieve a full length mitochondrial genome (mtDNA) assembly of *V. tsujii*, we partitioned and

269   assembled sequences separately from the nuclear genome. We mapped Illumina reads from

270   our Chromium libraries (Table S3) to the known mtDNA of the closest available relative, *Vargula*

271   *hilgendorfii* (NC_005306.1) [48] using bowtie2 (v2.3.3.1)[49] (parameters: --very-sensitive-local). We

272   then extracted read pairs with at least one read mapped from the resulting BAM file with

273   samtools (parameters: view -G 12), then name-sorted, extracted in FASTQ format (parameters:

274   samtools fastq) and input the reads into SPAdes (v3.11.1)[50] for assembly (parameters: --only-

275   assembler -k55,127). Inspection of the resulting assembly graph using Bandage (v.0.8.1)[51],

276   combined with a heuristic manual deletion of low coverage nodes (deletion of nodes with

277   coverage <200x, mean coverage ~250x) gave rise to two loops with sequence similarity to the

278   *V. hilgendorfii* mtDNA that both circularized through a single path (Supplementary Figure 1.8.1).

279   We then manually inspected this graph via a blastn(2.7.1+)[52] aligned against the *V. hilgendorfii*

280   mtDNA through SequenceServer (v1.0.11)[53] and visualized with the Integrated Genomics

281   Viewer (v2.4.5)[54]. We noted that the single circularizing path was homologous to the two

282   duplicated control regions reported in the *V. hilgendorfii* mtDNA [48]. We surmised that this

283   assembly graph structure indicated the *V. tsujii* mtDNA had the same global structure as the *V.*

284   *hilgendorfii* mtDNA, and so used the Bandage "specify exact path" tool to traverse the SPAdes

285   assembly graph and generate a FASTA file representing the circularized *V. tsujii* mtDNA with

286   the putative duplicated control regions (Figure S1). To avoid splitting sequence features across

287   the mtDNA circular sequence break, we circularly rotated this full assembly with the seqkit

288   (v0.7.2)[55] "restart" command, to set the first nucleotide of the FASTA file at the start codon of

289   ND2. We then confirmed 100% of the nucleotides via bowtie2 re-mapping of reads and

290   polishing with Pilon (v1.21)[56] (parameters: --fix all). We annotated the final assembly of the

291   mitochondrial genome using the MITOS2 web server [57] with the invertebrate mitochondrial

292   genetic code (translation table 5). We manually removed low confidence and duplicate gene

293   predictions from the MITOS2 annotation.

294

295   **Results**

296   *Population genetics analyses*

297   Our COI haplotype network revealed minimal structure among *V. tsujii* populations in southern

298   California (Figure 3A). Haplotypes from San Pedro and Catalina Island overlap or diverge by

299   only one to three mutations. Haplotypes from San Diego individuals, although still very similar to

300   haplotypes from Catalina Island and San Pedro, differ by at least eight mutations and show no

301   overlap with haplotypes from other populations of *V. tsujii*. However, the haplotype network for

302   16S indicates that sequences from San Diego individuals are identical to some individuals from

303   the other two populations. Furthermore, although the model with three clusters was favored in

13

304   the DAPC analysis for each gene (Supplementary Materials S2 and S3), membership in five of

305   the six clusters includes individuals from different populations (Supplementary Materials S4 and

306   S5). Therefore our analyses do not support three genetically distinct populations as defined by

307   location.
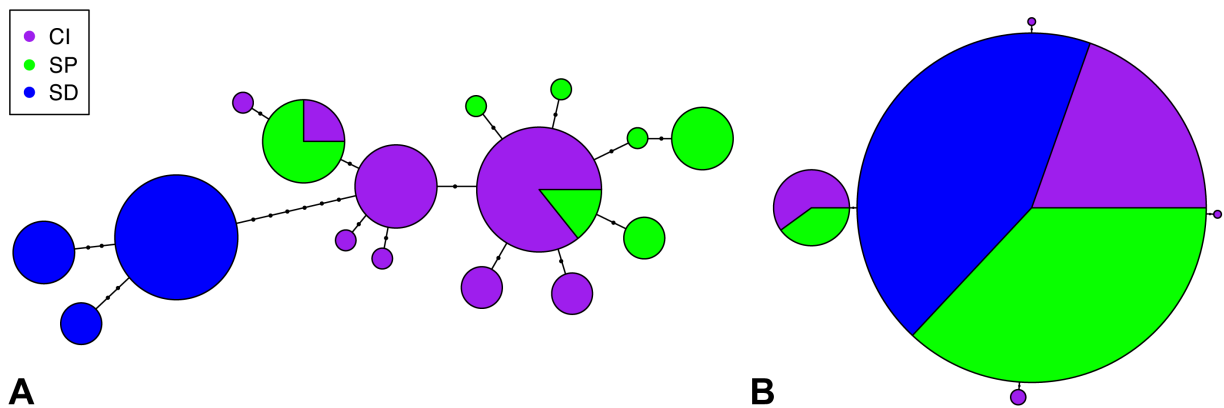
308

309

310

A **B**

311   **Figure 3.** Haplotype networks for (A) COI sequences, and (B) 16S sequences of Vargula tsujii animals from three localities sampled. Abbreviations: CI, Catalina Island; SD, San Diego; SP, San Pedro.

312

313   *Embryogenesis Description*

314   After fertilization and release into the marsupium, *V. tsujii* embryos resemble opaque, green,

315   ovoidal embryos (Figures 4 and 5). After five to eight days of growth, separation of the yolk

316   begins, which appears as a light green mass condenses within the embryo. Around ten to

317   eighteen days after deposition into the brooding chamber, two very small red lateral eyespots

318   are visible on each embryo and the separation of the yolk continues. Daily observations over the

319   next six days showed continual growth and darkening of the eyes. By day sixteen the yolk is

320   almost completely separated and has begun to form the gut of the ostracod. By days fifteen to

321   nineteen, the eyespots are mostly black and the light organ (a light brown/yellow mass) appears

322   anteroventral to the eyes of the embryo. Around twenty days after deposition, developing limbs

323   in the form of two rows of small brown masses are visible along the ventral side of the embryos.

14

324   At this point the gut has finished forming within the carapace and is visible as a yellow-white

325   mass on the posterior end of each embryo. Limb formation continues over the next few days,

326   and the eyes of each embryo become entirely black. Twenty-five to thirty-eight days following

327   embryo deposition, embryogenesis is complete, and instars are released from the mother's

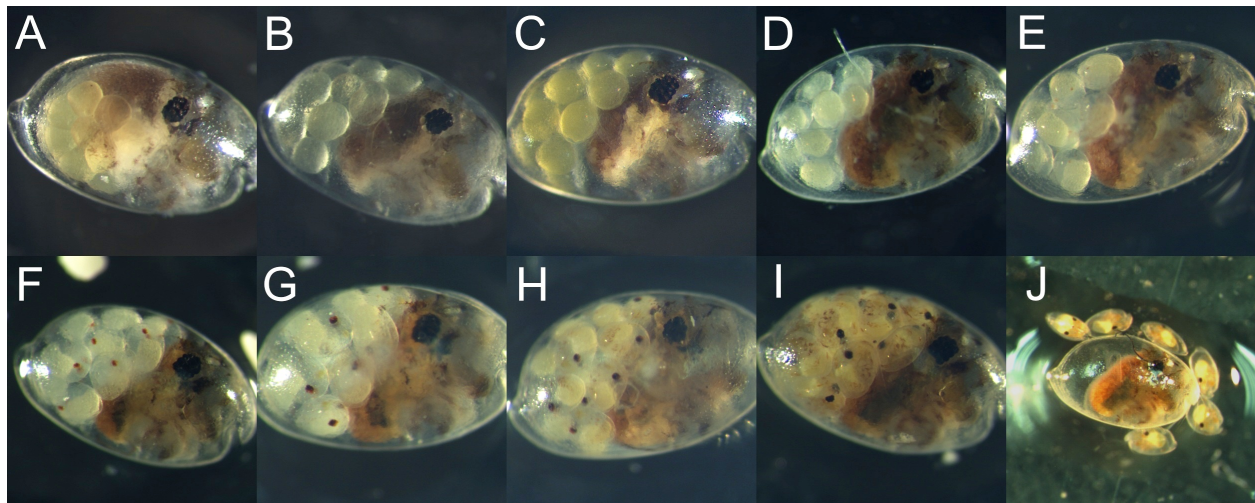328   marsupium.

329

330

331   **Figure 4.** Embryogenesis within brooding females of V. tsujii post release into the marsupium. (A) Day 0, (B) Day 1-4, (C) Day 5-7, (D) Day 8-9, (E) Day 10-13, (F) Day 14-17, (G) Day 18-19, (H) Day 20-21, (I) Day 22-23, (J) Day
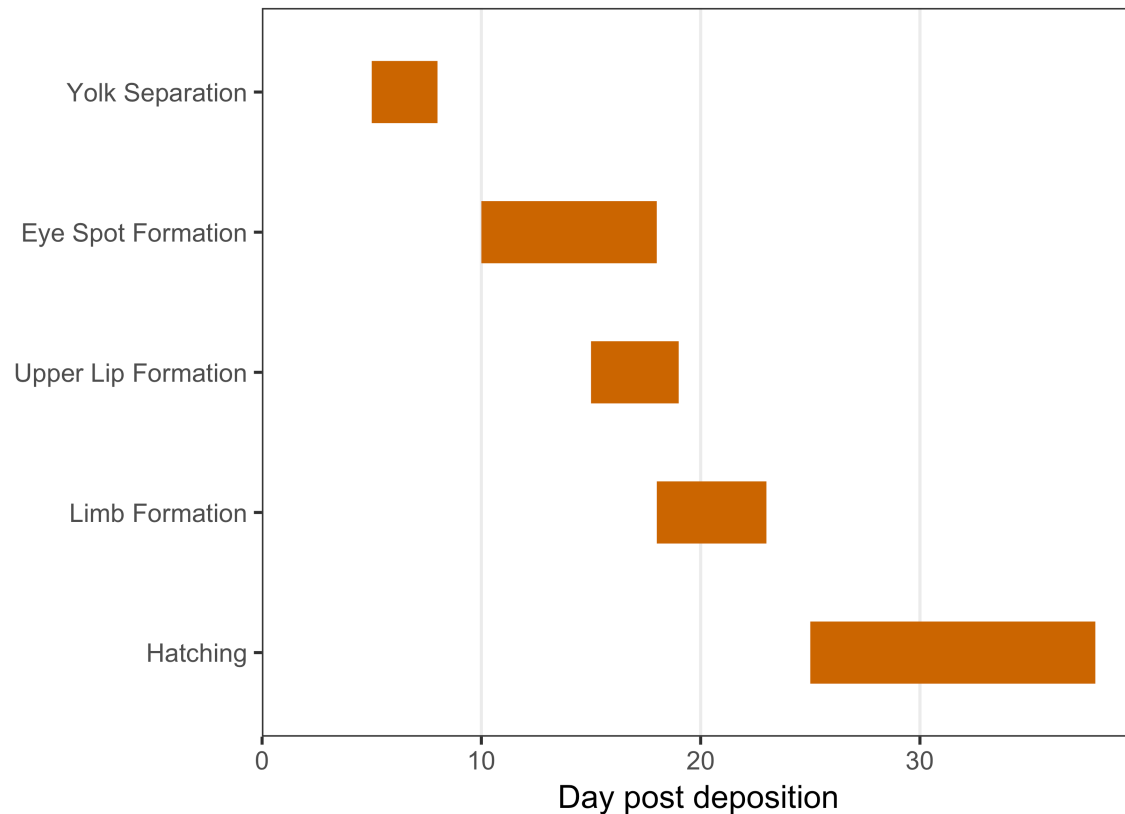332   25-39.

333

334

335

336

337

338

Figure 5. Summary of the timing of embryogenesis stages in V. tsujii. This represents the complete range of first appearance of each features across multiple broods, including: yolk separation (range = 5-8 days, N = 7); eye spot formation (range = 10-18 days, N = 12); upper lip formation (range = 15-19 days, N = 3); limb formation (range = 18-23 days, N = 11); hatching (range = 25-38 days, N = 11).

Instar development

Vargula tsujii has five inferred juvenile instar stages (A-I, A-II, A-III, A-IV, A-V) and an adult

stage, most of which have a conserved size range (Figure 6A; Table 3). Laboratory

measurements of specimens of unknown sex were compared with the measurements of sexed

individuals (9 males, 11 females) to confirm interpretation of the instar stage of size classes

(Figure 6C-D). Due to large amounts of overlap of A-1 females with adult and A-I males, these

three groups are currently indistinguishable in our data set. Sexual dimorphism becomes

apparent in adulthood, with adult females clearly larger than adult males. However, compared to

many other cypridinid ostracods, this dimorphism can be difficult to assess visually without a

side-by-side comparison.

Evidence for complete life cycle in the lab

16

353 To assess whether a complete life cycle was obtained in the laboratory, we began with only

354 brooding females in a small experimental aquarium. Those brooding females, although not

355 tracked individually, released a number of juveniles, which we measured intermittently over time

356 (Figure 6B). In this aquarium we found juveniles, and eventually adults, that fell across the full

357 size range of wild-caught ostracods. After all of the broods hatched, we removed all adult

358 females from the experimental aquarium to assess whether the ostracods would mature and

359 mate in the laboratory. Following removal of the original adult females, we found adult brooding

360 females that grew up in experimental aquarium that themselves gave birth to the next

361 generation in 3-4 months time.

362
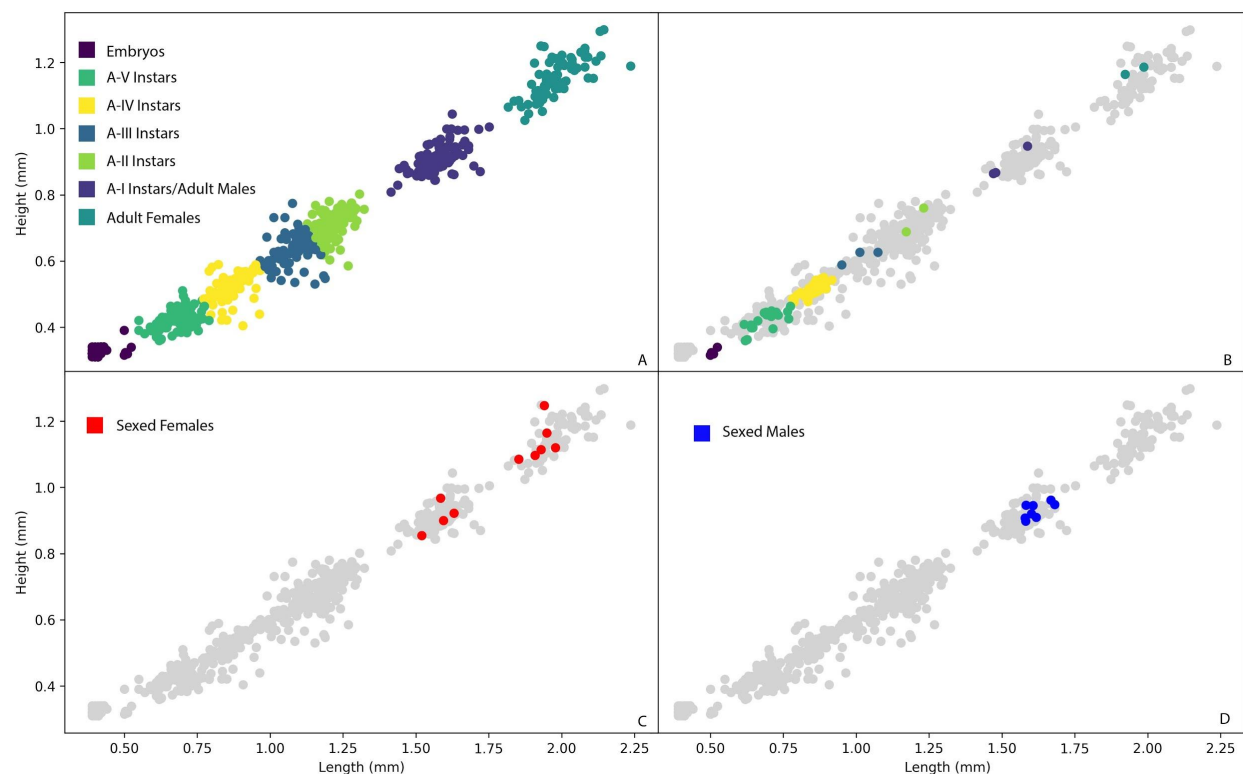
Figure 6. (A) K-means clusters of Vargula tsujii developmental stages based on carapace height and width. Instar stages were assigned to each cluster via comparison to P. annecohenae and additional analysis of male and female size dimorphism. (B) Points representing laboratory cultured animals overlayed on wild caught and unknown data. Different colors represent different clusters in the k-means analysis, and are labeled with their inferred instar/adult stages. (C) Shows wild-caught animals dissected and identified as female in relation to the k-means clusters, and (D) shows wild-caught animals dissected and identified as male in relation to the k-means clusters.

367

17

368   *Nuclear and mitochondrial genome assemblies*

369   Our final *Vargula tsujii* nuclear genome assembly is highly fragmented, with an indication of high

370   levels of heterozygosity between haplotypes (~5%) and a high proportion of simple sequence

371   repeats. Our post-sequencing analysis indicated the mode of the DNA size distribution for the

372   four extracted DNA samples were 1244 bp, 3820 bp, 1285 bp (sample #5047), and 1279 bp,

373   respectively, with a tail of ~20-40 kbp in each sample.

374

375   The final *V. tsujii* mtDNA (15,729 bp) (Figure 7) aligned to the previously published *V.*

376   *hilgendorfii* mtDNA [48] with 98% coverage and 78.5% nucleotide identity, and is available on

377   NCBI GenBank (MG767172). The *V. tsujii* mtDNA contains 22 tRNA genes, 13 protein coding

378   genes, and 2 duplicated control regions in an identical positioning and orientation to the *V.*

379   *hilgendorfii* mtDNA. There is one polymorphic base in the final mitogenome assembly coding for

380   a synonymous wobble mutation in the COII gene (COII:L76).

381
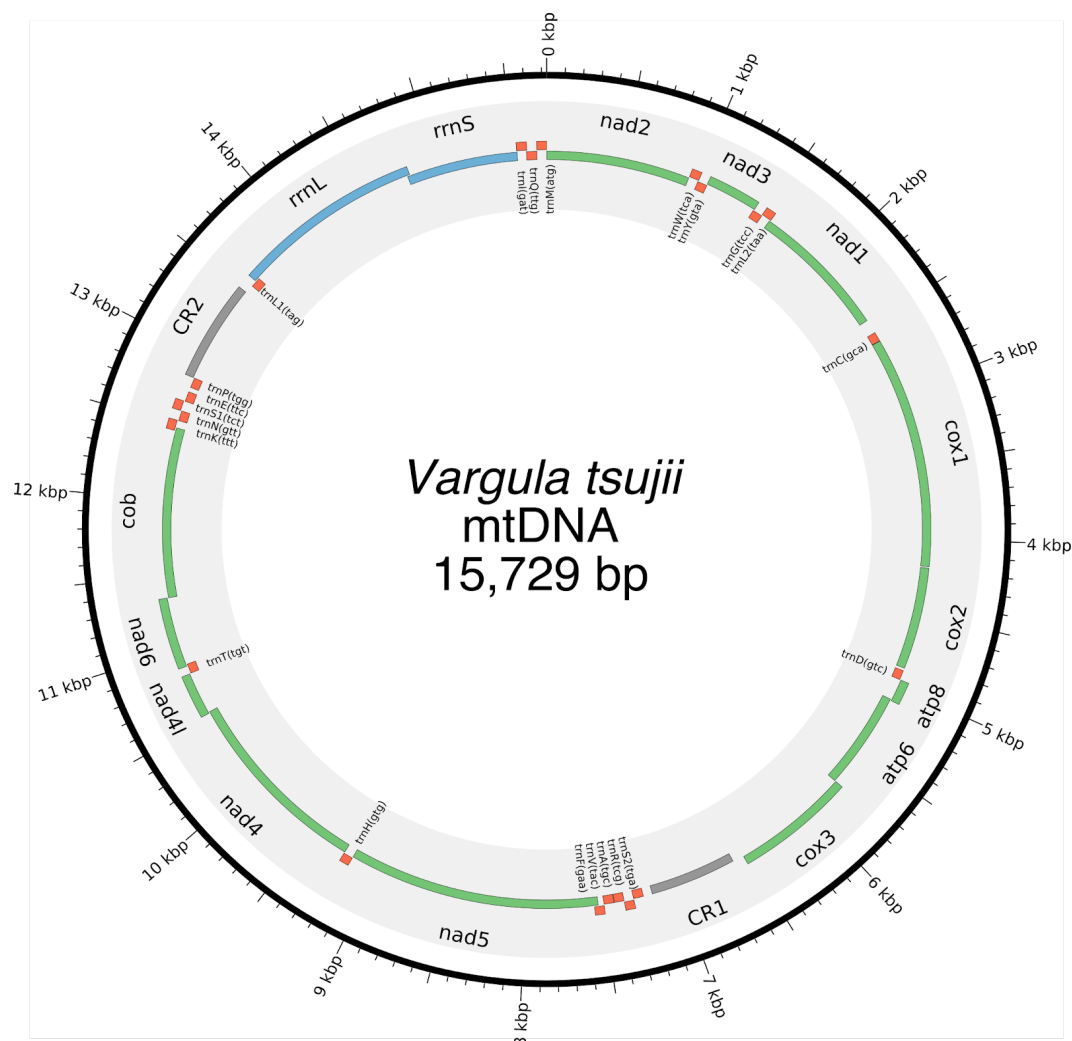
Figure 7. Mitochondrial genome of V. tsujii. Note the duplicated control regions, CR1 and CR2 (in gray). Figure produced with Circos [80].

Discussion

Based on measurement data on the first and second generations of ostracods reared in the lab (Figure 5), and the presence of brooding female ostracods in our experimental aquarium where adult females had previously been removed, we can infer that we were successful in rearing *Vargula tsujii* through its complete life cycle in the lab. This is a first for any bioluminescent ostracod, as rearing in the lab has remained a significant hurdle for laboratory studies in these animals [26–28]. Our current population was cultured from animals collected near Wrigley Marine Science Center on Santa Catalina Island, which appears to contain much of the genetic

393   diversity sampled across much of the known the range of *V. tsujii* (Figure 3). Our population

394   genetics analyses support the hypothesis that populations of *Vargula tsujii* experience some

395   gene flow across the localities sampled, including Catalina Island. These results are consistent

396   with the hypothesis that *V. tsujii* represents a single, connected species. As such, we assume

397   our culture of ostracods from Santa Catalina Island, and inferences made from it, may be

398   representative of the genetic diversity of populations of *V. tsujii* across southern California

399   coastal systems. However, we cannot discount the possibility that there might be some variation

400   in development times and instar sizes across the range of this species. Also of note is that this

401   species is not easily collected throughout the reported range, and northern populations, if they

402   exist, may be divergent from southern California populations.

403

404   *Attempted whole genome reconstruction*

405   The 1C genome size of *Vargula tsujii* was previously reported to be 4.46 ± 0.08 pg (Female,

406   n=3), and 4.05 pg (Male, n=1) [58], corresponding to a 1C genome size of 4.36 Gbp and 3.96 Gbp

407   respectively and suggesting XO sex determination. Our reconstruction of the *Vargula tsujii*

408   nuclear genome assembly is highly fragmented, with an indication of high levels of

409   heterozygosity between haplotypes (~5%) and a high proportion of simple sequence repeats.

410   We speculate that our poor nuclear genome assembly results are likely due to the small size

411   distribution of the input DNA, as larger fragment sizes are especially critical for the

412   reconstruction of large genomes such as *V. tsujii*. Further protocol development is needed to

413   extract suitable High Molecular Weight DNA, which could allow long-read sequencing that would

414   improve assembly.

415

416   *The life cycle of* Vargula tsujii

417   The embryogenesis of *Vargula tsujii* is similar to closely related species, and the 24-day

418   average brooding duration falls within the range for other cypridinid ostracods (10-30 days) [59].

20

419   The primary stages of *V. tsujii* embryonic development are yolk separation, formation of eye

420   spots, development of the upper lip, development of limbs, and emergence from the chorion and

421   marsupium (Figure 5). In general, the embryonic development of *Vargula tsujii* is longer than

422   that of other luminescent ostracods whose development has been described (Table 4).

423   However, early embryonic development in *V. tsujii* is faster than in *P. annecohenae*. In *P.*

424   *anncohenae,* yolk separation begins on day 9 and eye development begins on days 14-15 [27],

425   while those stages begin at 5-7 and 10-13 days, respectively, in *V. tsujii*. Additionally, the order

426   of development in *V. tsujii* appears to differ from that of *Vargula hilgendorfii,* which starts to

427   develop limbs on days 4-5, before eye and upper lip development [27,60]. By contrast, *V. tsujii* limbs

428   do not appear until after eye-spot and upper lip formation. The reasons for this difference are

429   unclear.

430

431   Juvenile development of *Vargula tsujii* is also quite similar overall to that of *Photeros*

432   *annecohenae*, the only other bioluminescent cypridinid ostracod for which instar developmental

433   data is available [27]. We inferred five distinct instar stages (A-V through A-I), and A-I instars

434   develop into size dimorphic adult males and females (Table 3). Average measurements of size,

435   including carapace length and height, as well as eye width, were comparable between

436   respective instar stages in *V. tsujii* and *P. annecohenae*. However, in *V. tsujii* average eye width

437   remains within the range of 0.060 mm to 0.0684 mm from the embryonic stage until the second

438   instar, and makes a large jump by about two fold in the third instar (0.121 ± 0.0208 mm), as

439   compared to a gradual increase in eye size in *P. annecohenae*. In our k-means clustering

440   analysis, the second-to-largest cluster of *V. tsujii* appears to contain adult males as well as A-I

441   males and females. This finding differs from that in *P. annecohenae*, where adult males were

442   found to cluster separately from A-I males and females and adult females based on size and

443   shape, and A-I males and females could be distinguished by certain shape parameters [27]. We

444   hypothesize that this apparent reduction of sexual dimorphism observed in the later stages of

21

445   development may occur because *V. tsujii* may have lost the ability to use luminescence for

446   courtship, so selection acting on differences in male and female shape may have been reduced.

447

448   *Benefits of completing the life cycle*

449   Cypridinid ostracods represent an independent origin of endogenous autogenic

450   bioluminescence. This group is a natural comparison to other, well-studied bioluminescent

451   courtship systems, such as that of fireflies [61]. Other possible laboratory models for

452   bioluminescence, such as brittle stars [62] and cnidarians [63] are useful for some research tasks,

453   such as studies of luciferins obtained from the diet (e.g., coelenterazine). Others might be easier

454   to rear in the laboratory, such as the self-fertilizing brittle star *Amphiolus squamata* [64]. However,

455   ostracods produce their own luciferase and luciferin, unlike brittle stars and cnidarians.

456   Ostracods also have relatively fast generation times (on the order of months), which can be

457   modified somewhat by adjusting the temperature of the water, as is common among ostracods

458   [26–28,65,66]. In comparison, fireflies are usually on a six-month to one-year life cycle that is difficult to

459   alter [67–69], and some brittle stars appear to spawn only seasonally [70,71]. Furthermore, culture of an

460   organism (*Vargula tsujii*) from a clade with an independent origin of autogenic bioluminescence

461   allows for comparative studies between luminescence in ostracods and the autogenic

462   bioluminescence found in fireflies [16] or other organisms, which would not otherwise be possible.

463

464   Ostracods will be incredibly useful for studying the physiology and biochemistry of

465   bioluminescence [2], as both diversification and behavioral changes in cypridinids related to

466   luminescence have occurred using the same luciferin and homologous luciferases [24].

467   Furthermore, ostracod courtship signals are bright and easily simulated in a laboratory setting,

468   allowing for assessments of male and female behavior in response to changes in signal

469   parameters, such as intensity, color, and pulse duration (e.g., [72]). These tools provide

470   researchers with an excellent system for asking important questions related to selection on

22

471   genes important for rapid diversification [73], including those related to behavior [74], sexual selection

472   [75], and the role of the biochemical properties of bioluminescence [25].

473

474   Importantly, the biosynthetic pathway for luciferin production is currently unknown for any animal

475   system. One major obstacle to describing this pathway has been building laboratory cultures for

476   animal species that produce luciferin themselves and also have a relative fast generation time.

477   Solving this bottleneck to accessing specimens for bioluminescent ostracods has set the stage

478   for investigations into the biosynthetic pathway of cypridinid luciferin and its possible use in

479   biomedical tools such as optogenetics [76]. Finally, this is an excellent system with which to

480   consider developing genome editing techniques (e.g., CRISPR/Cas9) [77] to test candidate genes

481   for luciferin biosynthesis, and to assess how genetic variants in critical genes might affect

482   production or perception of bioluminescent signals.

483

484   **Acknowledgements**

495

496

Author contributions

JAG, ET, JKW, and THO conceived of and designed the study; JAG, GM, MNB, MSD, JDM, TRF, and DTS contributed to the acquisition and analysis of the data in this study; all authors participated in the interpretation of data, helped draft or substantially revise the manuscript, and gave final approval for publication.

Competing interests

The authors declare no competing interests.

Data availability

Sequence data for COI and 16S are available in GenBank (Table S1) and our whole genome Chromium reads are available in the Sequence Read Archive (SRR9308458). Scripts and data for the population genetics and k-means clustering analyses are provided on Github (https://github.com/goodgodric28/vargula_tsujii_culture). An additional video which shows *Vargula tsujii* hatching from the chorion and outside the mother is provided on Youtube (https://youtu.be/8o5CqHTcTjI).

References

1. Haddock, S. H. D., Moline, M. A. & Case, J. F. Bioluminescence in the sea. *Ann. Rev. Mar. Sci.* **2**, 443–493 (2010).

2. Hastings, J. W. Biological diversity, chemical mechanisms, and the evolutionary origins of bioluminescent systems. *J. Mol. Evol.* **19**, 309–321 (1983).

3. Shimomura, O., Johnson, F. H. & Saiga, Y. Extraction, purification and properties of aequorin, a bioluminescent protein from the luminous hydromedusan, *Aequorea*. *J. Cell. Comp. Physiol.* **59**, 223–239 (1962).

24

522   4. Tsuji, F. I. ATP-dependent bioluminescence in the firefly squid, *Watasenia scintillans*. *Proc.*

523   *Natl. Acad. Sci. U. S. A.* **82**, 4629–4632 (1985).

524   5. Cormier, M. J., Wampler, J. E., Hori, K. & Lee, J. W. Bioluminescence of *Renilla reniformis*.

525   IX. Structured bioluminescence. Two emitters during both the in vitro and the in vivo

526   bioluminescence of the sea pansy, *Renilla*. *Biochemistry* **10**, 2903–2909 (1971).

527   6. Dunlap, P. Biochemistry and Genetics of Bacterial Bioluminescence in *Advances in*

528   *Biochemical Engineering/Biotechnology* 37–64 (2014).

529   7. Fallon, T. R. *et al.* Firefly genomes illuminate parallel origins of bioluminescence in beetles.

530   *Elife* **7**, (2018).

531   8. Sweeney, B. The Bioluminescence of Dinoflagellates in *Biochemistry and Physiology of*

532   *Protozoa* 287–306 (1979).

533   9. Kobayashi, K. *et al.* Purification and properties of the luciferase from the marine ostracod

534   *Vargula hilgendorfii* in *Bioluminescence and Chemiluminescence* (2001).

535   doi:10.1142/9789812811158_0022

536   10. Hastings, J. W., Vergin, M. & Desa, R. Scintillons: The Biochemistry of Dinoflagellate

537   Bioluminescence in *Bioluminescence in Progress* 301–330 (Princeton University Press,

538   1967).

539   11. Nakatsu, T. *et al.* Structural basis for the spectral difference in luciferase bioluminescence.

540   *Nature* **440**, 372–376 (2006).

541   12. Marques, S. M. & Esteves da Silva, J. C. G. Firefly bioluminescence: a mechanistic

542   approach of luciferase catalyzed reactions. *IUBMB Life* **61**, 6–17 (2009).

543   13. Verhaegent, M. & Christopoulos, T. K. Recombinant *Gaussia* luciferase. Overexpression,

544   purification, and analytical application of a bioluminescent reporter for DNA hybridization.

545   *Anal. Chem.* **74**, 4378–4385 (2002).

546   14. Dunlap, P. V. & Urbanczyk, H. Luminous Bacteria. *The Prokaryotes* 495–528 (2013).

547   doi:10.1007/978-3-642-30141-4_75

548   15. Kotlobay, A. A. *et al.* Genetically encodable bioluminescent system from fungi. *Proc. Natl.*

549   *Acad. Sci. U. S. A.* **115**, 12728–12732 (2018).

550   16. Kanie, S., Nakai, R., Ojika, M. & Oba, Y. 2-S-cysteinylhydroquinone is an intermediate for

551   the firefly luciferin biosynthesis that occurs in the pupal stage of the Japanese firefly, *Luciola*

552   *lateralis*. *Bioorg. Chem.* **80**, 223–229 (2018).

553   17. McLean, M., Buck, J. & Hanson, F. E. Culture and larval behavior of photurid fireflies. *Am.*

554   *Midl. Nat.* **87**, 133 (1972).

555   18. Thompson, E. M., Nagata, S. & Tsuji, F. I. Cloning and expression of cDNA for the luciferase

556   from the marine ostracod *Vargula hilgendorfii*. *Proc. Natl. Acad. Sci. U. S. A.* **86**, 6567–6571

557   (1989).

558   19. Oba, Y., Kato, S.-I., Ojika, M. & Inouye, S. Biosynthesis of luciferin in the sea firefly,

559   *Cypridina hilgendorfii*: l-tryptophan is a component in *Cypridina* luciferin. *Tetrahedron Lett.*

560   **43**, 2389–2392 (2002).

561   20. de Wet, J. R., Wood, K. V., Helinski, D. R. & DeLuca, M. Cloning of firefly luciferase cDNA

562   and the expression of active luciferase in *Escherichia coli*. *Proc. Natl. Acad. Sci. U. S. A.* **82**,

563   7870–7873 (1985).

564   21. Seliger, H. H., McElroy, W. D., White, E. H. & Field, G. F. Stereo-specificity and firefly

565   bioluminescence, a comparison of natural and synthetic luciferins. *Proc. Natl. Acad. Sci. U.*

566   *S. A.* **47**, 1129–1134 (1961).

567   22. Morin, J. G. Luminaries of the reef: The history of luminescent ostracods and their courtship

568   displays in the Caribbean. *Journal of Crustacean Biology* **39**, 227–243 (2019).

569   23. Cohen, A. C. & Morin, J. G. Sexual morphology, reproduction and the evolution of

570   bioluminescence in Ostracoda. *Paleontological Society Papers* **9**, 37 (2003).

571   24. Morin, J. G. Based on a review of the data, use of the term 'cypridinid' solves the

572   *Cypridina/Vargula* dilemma for naming the constituents of the luminescent system of

573   ostracods in the family cypridinidae. *Luminescence* **26**, (2011).

574   25. Hensley, N. M. *et al.* Phenotypic evolution shaped by current enzyme function in the

575   bioluminescent courtship signals of sea fireflies. *Proc. R. Soc. B* **286**, 20182621 (2019).

576   26. Cohen, A. C. Rearing and postembryonic development of the myodocopid ostracode

577   *Skogsbergia lerneri* from coral reefs of Belize and the Bahamas. *J. Crustacean Biol.* **3**, 235–

578   256 (1983).

579   27. Gerrish, G. A. & Morin, J. G. Life Cycle of a Bioluminescent Marine Ostracode, *Vargula*

580   *annecohenae* (Myodocopida: Cypridinidae). *J. Crustacean Biol.* **28**, 669–674 (2008).

581   28. Wakayama, K & Kanazawa, K. Elucidation of environmental tolerance of sea fireflies and

582   research on construction of optimal rearing environment *Sci. J. Kangawa U.* **25**, 117-124

583   (2014).

584   29. Pérez-Lloréns, J. L. Cooking-Science-Communication (CSC): The ideal trident to enjoy the

585   dining experience. *International Journal of Gastronomy and Food Science* **16**, 100134

586   (2019).

587   30. Koyama, K. H. & Rivera, A. S. Embryonic development of the myodocopid ostracod

588   *Euphilomedes carcharodonta* Smith, 1952. *J. Crustacean Biol.* (2018).

589   doi:10.1093/jcbiol/ruy088

590   31. Kawamata, K., Sato, M. & Abe, K. Complete life cycle of the ostracod *Euphilomedes*

591   *nipponica* (Myodocopida, Philomedidae). *Plankton Benthos Res.* **13**, 83–89 (2018).

592   32. Ikeya, N. & Kato, M. The life history and culturing of *Xestoleberis hanaii* (Crustacea,

593   Ostracoda) in *Evolutionary Biology and Ecology of Ostracoda* (eds. Horne, D. J. & Martens,

594   K.) 149–159 (Springer Netherlands, 2000).

595   33. Korniker, L. S. & Baker, J. H. *Vargula tsujii*, a new species of luminescent ostracod from

596   lower and southern California (Myodocopa: Cypridininae). *Proceedings of the Biological*

597   *Society of Washington* **90**, 218–231 (1977).

598   34. Hammer, R. M. Day-night differences in the emergence of demersal zooplankton from a

599   sand substrate in a kelp forest. *Mar. Biol.* **62**, 275–280 (1981).

600   35. Stepien, C. A. & Brusca, R. C. Nocturnal attacks on nearshore fishes in southern California

601   by crustacean zooplankton. *Marine Ecology Progress Series* **25**, 91–105 (1985).

602   36. Warner, J. A. & Case, J. F. The zoogeography and dietary induction of bioluminescence in

603   the midshipman fish, *Porichthys notatus*. *The Biological Bulletin* **159**, 231–246 (1980).

604   37. Cohen, A. C. & Oakley, T. H. Collecting and processing marine ostracods. *J. Crustacean*

605   *Biol.* **37**, 347–352 (2017).

606   38. Lee, K. H.-H. Genetic differentiation in *Vargula tsujii* (Ostracoda: Cypridinidae) along the

607   California coast. (California State University, Los Angeles, 2002).

608   39. Paradis, E. pegas: an R package for population genetics with an integrated-modular

609   approach. *Bioinformatics* **26**, 419–420 (2010).

610   40. R Core Team. R: A Language and Environment for Statistical Computing. (2017).

611   41. Jombart, T. adegenet: a R package for the multivariate analysis of genetic markers.

612   *Bioinformatics* **24**, 1403–1405 (2008).

613   42. Schwarz, G. Estimating the Dimension of a Model. *Ann. Stat.* **6**, 461–464 (1978).

614   43. Vannier, J., Abe, K. & Ikuta, K. Feeding in myodocopid ostracods: functional morphology

615   and laboratory observations from videos. *Mar. Biol.* **132**, 391–408 (1998).

616   44. Schindelin, J. *et al.* Fiji: an open-source platform for biological-image analysis. *Nat. Methods*

617   **9**, 676–682 (2012).

618   45. Pedregosa, F. *et al.* Scikit-learn: Machine Learning in Python. *J. Mach. Learn. Res.* **12**,

619   2825–2830 (2011).

620   46. Van Rossum, G. & Drake, F. L., Jr. *Python tutorial*. (Centrum voor Wiskunde en Informatica

621   Amsterdam, 1995).

622   47. Weisenfeld, N. I., Kumar, V., Shah, P., Church, D. M. & Jaffe, D. B. Direct determination of

623   diploid genome sequences. *Genome Res.* **27**, 757–767 (2017).

624   48. Ogoh, K. & Ohmiya, Y. Complete mitochondrial DNA sequence of the sea-firefly, *Vargula*

625   *hilgendorfii* (Crustacea, Ostracoda) with duplicate control regions. *Gene* **327**, 131–139

626   (2004).

627   49. Langmead, B. & Salzberg, S. L. Fast gapped-read alignment with Bowtie 2. *Nat. Methods* **9**,

628   357–359 (2012).

629   50. Nurk, S. *et al.* Assembling Genomes and Mini-metagenomes from Highly Chimeric Reads. in

630   *Lecture Notes in Computer Science* 158–170 (2013).

631   51. Wick, R. R., Schultz, M. B., Zobel, J. & Holt, K. E. Bandage: interactive visualization of de

632   novo genome assemblies. *Bioinformatics* **31**, 3350–3352 (2015).

633   52. Camacho, C. *et al.* BLAST+: architecture and applications. *BMC Bioinformatics* **10**, 421

634   (2009).

635   53. Priyam, A. *et al.* Sequenceserver: a modern graphical user interface for custom BLAST

636   databases. *bioRxiv* 033142 (2015). doi:10.1101/033142

637   54. Robinson, J. T. *et al.* Integrative genomics viewer. *Nat. Biotechnol.* **29**, 24–26 (2011).

638   55. Shen, W., Le, S., Li, Y. & Hu, F. SeqKit: A Cross-Platform and Ultrafast Toolkit for FASTA/Q

639   File Manipulation. *PLoS One* **11**, e0163962 (2016).

640   56. Walker, B. J. *et al.* Pilon: an integrated tool for comprehensive microbial variant detection

641   and genome assembly improvement. *PLoS One* **9**, e112963 (2014).

642   57. Bernt, M. *et al.* MITOS: improved de novo metazoan mitochondrial genome annotation. *Mol.*

643   *Phylogenet. Evol.* **69**, 313–319 (2013).

644   58. Jeffery, N. W., Ellis, E. A., Oakley, T. H. & Gregory, T. R. The genome sizes of ostracod

645   crustaceans correlate with body size and evolutionary history, but not environment. *J.*

646   *Hered.* **108**, 701–706 (2017).

647   59. Cohen, A. C. & Morin, J. G. Patterns of reproduction in ostracodes: a review. *Journal of*

648   *Crustacean Biology* **10**, 184 (1990).

649   60. Wakayama, N. Embryonic development clarifies polyphyly in ostracod crustaceans. *Journal*

650   *of Zoology* **273**, 406–413 (2007).

651   61. Lewis, S. M. & Cratsley, C. K. Flash signal evolution, mate choice, and predation in fireflies.

652   *Annu. Rev. Entomol.* **53**, 293–321 (2008).

653   62. Deheyn, D. D. Bioluminescence in the brittle star *Amphipholis squamata* (echinodermata):

654   an overview of 10 years of research. in *Bioluminescence and Chemiluminescence* (2001).

655   doi:10.1142/9789812811158_0009

656   63. Houliston, E., Momose, T. & Manuel, M. *Clytia hemisphaerica*: a jellyfish cousin joins the

657   laboratory. *Trends Genet.* **26**, 159–167 (2010).

658   64. Boissin, E., Hoareau, T. B., Féral, J. P. & Chenuil, A. Extreme selfing rates in the

659   cosmopolitan brittle star species complex *Amphipholis squamata*: data from progeny-array

660   and heterozygote deficiency. *Mar. Ecol. Prog. Ser.* **361**, 151–159 (2008).

661   65. Heip, C. The life-cycle of *Cyprideis torosa* (Crustacea, Ostracoda). *Oecologia* **24**, 229–245

662   (1976).

663   66. Martens, K. Effects of temperature and salinity on postembryonic growth in *Mytilocypris*

664   *henricae* (Chapman) (Crustacea, Ostracoda). *Journal of Crustacean Biology* **5**, 258–272

665   (1985).

666   67. Viviani, V. R. Fireflies (Coleoptera: Lampyridae) from southeastern Brazil: habitats, life

667   history, and bioluminescence. *Ann. Entomol. Soc. Am.* **94**, 129–145 (2001).

668   68. Ho, J.-Z., Chiang, P.-H., Wu, C.-H. & Yang, P.-S. Life cycle of the aquatic firefly *Luciola ficta*

669   (Coleoptera: Lampyridae). *J. Asia. Pac. Entomol.* **13**, 189–196 (2010).

670   69. Fu, X., Nobuyoshi, O., Vencl, F. V. & Lei, C. Life cycle and behaviour of the aquatic firefly

671   *Luciola leii* (Coleoptera: Lampyridae) from Mainland China. *Can. Entomol.* **138**, 860–870

672   (2006).

673   70. Soong, K., Lin, Y., Chao, S. & Chang, D. Spawning time of two shallow-water brittle stars.

674   *Mar. Ecol. Prog. Ser.* **376**, 165–171 (2009).

675   71. Hagman, D. K. & Vize, P. D. Mass spawning by two brittle star species, *Ophioderma*

676   *rubicundum* and *O. Squamosissimum* (Echinodermata: Ophiuroidea), at the Flower Garden

677   Banks, Gulf of Mexico. *Bull. Mar. Sci.* **72**, 871–876 (2003).

678   72. Rivers, T. J. & Morin, J. G. Female ostracods respond to and intercept artificial conspecific

679   male luminescent courtship displays. *Behav. Ecol.* **24**, 877–887 (2013).

680   73. Stern, D. L. & Orgogozo, V. Is Genetic Evolution Predictable? *Science* **323**, 746–751 (2009).

681   74. Boake, C. R. B. *et al.* Genetic Tools for Studying Adaptation and the Evolution of Behavior.

682   *The American Naturalist* **160**, S143 (2002).

683   75. Ritchie, M. G. Sexual Selection and Speciation. *Annu. Rev. Ecol. Evol. Syst.* **38**, 79–102

684   (2007).

685   76. Yeh, H.-W. & Ai, H.-W. Development and applications of bioluminescent and

686   chemiluminescent reporters and biosensors. *Annu. Rev. Anal. Chem.* (2019).

687   doi:10.1146/annurev-anchem-061318-115027

688   77. Cong, L. *et al.* Multiplex genome engineering using CRISPR/Cas systems. *Science* **339**,

689   819–823 (2013).

690   78. Krzywinski, M. *et al.* Circos: an information aesthetic for comparative genomics. *Genome*

691   *Res.* **19**, 1639–1645 (2009).

692   79. Pang, K. & Martindale, M. Q. Mnemiopsis leidyi Spawning and Embryo Collection. *CSH*

693   *Protoc.* **2008**, db.prot5085 (2008).

694   80. Warren, K. J. The establishment and characterization of primary cell cultures derived from

695   the ctenophore *Mnemiopsis leidyi*. (University of Miami, 2016).

696   81. Baker, L. D. & Reeve, M. R. Laboratory culture of the lobate ctenophore *Mnemiopsis*

697   *mccradyi* with notes on feeding and fecundity. *Marine Biology* **26**, 57–62 (1974).

698   82. Kahn, B. Scientists Have Cultivated a Mesmerizing Jelly That's Like 'Barely Organized

699   Water'. *Earther* (2018). Available at: https://earther.gizmodo.com/scientists-have-cultivated-

700   a-mesmerizing-jelly-thats-li-1823207295. (Accessed: 28th June 2019)

701   83. Lindner, A. & Migotto, A. E. The life cycle of *Clytia linearis* and *Clytia noliformis*: metagenic

702   campanulariids (Cnidaria: Hydrozoa) with contrasting polyp and medusa stages. *Journal of*

703   *the Marine Biological Association of the United Kingdom* **82**, 541–553 (2002).

704   84. Delroisse, J., Ortega-Martinez, O., Dupont, S., Mallefet, J. & Flammang, P. De novo

705   transcriptome of the European brittle star *Amphiura filiformis* pluteus larvae. *Mar. Genomics*

706   **23**, 109–121 (2015).

707   85. Oba, Y. *et al.* Bioluminescence of a firefly pupa: involvement of a luciferase isotype in the

708   dim glow of pupae and eggs in the Japanese firefly, *Luciola lateralis. Photochem. Photobiol.*

709   *Sci.* **12**, 854–863 (2013).

710   86. Watkins, O. C., Sharpe, M. L., Perry, N. B. & Krause, K. L. New Zealand glowworm

711   (*Arachnocampa luminosa*) bioluminescence is produced by a firefly-like luciferase but an

712   entirely new luciferin. *Sci. Rep.* **8**, 3278 (2018).

713   87. Meyer-Rochow, V. B. Glowworms: a review of *Arachnocampa* spp. and kin. *Luminescence*

714   **22**, 251–265 (2007).

715   88. Takaie, H. Ten years of the glow-worm (*Arachnocampa richardsae*) rearing at Tama Zoo--

716   Fascination of a living milky way. *Insectarium* **34**, 336–342 (1997).

717   89. Maheswarudu, G. & Vineetha, A. Culture of the littoral oligochaete *Pontodrilus bermudensis*

718   Beddard. *The Journal of Bioprocess Technology* **97**, 142–155 (2013).

719   90. Nishida, H. Development of the appendicularian *Oikopleura dioica*: culture, genome, and

720   cell lineages. *Dev. Growth Differ.* **50 Suppl 1**, S239–56 (2008).

721   91. Martí-Solans, J. *et al. Oikopleura* dioica culturing made easy: a low-cost facility for an

722   emerging animal model in EvoDevo. *Genesis* **53**, 183–193 (2015).

723

724

725

726

727

728

729   **Figures**

730   **Figure 1.** Map of localities where collections (and attempted collections of *Vargula tsujii* were

731   made). Black points represent geographic annotations for reference, purple points refer to the

732   location where ostracods were collected that were ultimately cultured, blue where animals were

733   found or collected, orange where Kornicker originally collected animals, and red where no *V.*

734   *tsujii* were found. (A) Map of the California (USA) coastline where *V. tsujii* collections were

735   attempted; (B) Map of the region near Two Harbors (Santa Catalina Island, California, USA)

736   where *V. tsujii* collections were attempted.

737

738   **Figure 2.** Diagrammatic representation of aquarium setup for sea fireflies. (A) Source water

739   flows into (B) a reservoir tank, which overflows to keep the reservoir full and water level

740   constant. (C) We use a siphon to carry water from a reservoir tank to main aquarium where

741   ostracods live. Water level of the main tank drains through sand (stippled), through (E) an

742   outflow that is raised to a level that would cause water to remain at the level of the dashed line,

743   even if a siphon is interrupted to cause water to stop flowing into the main tank. (F) Plastic bottle

744   and parts used to create small aquarium using the same logic as main aquarium. (G) Custom-

745   built acrylic aquarium with drain in bottom and raised outflow with adjustable rate.

746

747   **Figure 3.** Figure 3. Haplotype networks for (A) COI sequences, and (B) 16S sequences of

748   *Vargula tsujii* animals from three localities sampled. Abbreviations: CI, Catalina Island; SD, San

749   Diego; SP, San Pedro.

750

751   **Figure 4.** Embryogenesis within brooding females of *V. tsujii* post release into the marsupium.

752   (A) Day 0, (B) Day 1-4, (C) Day 5-7, (D) Day 8-9, (E) Day 10-13, (F) Day 14-17, (G) Day 18-19,

753   (H) Day 20-21, (I) Day 22-23, (J) Day 25-38.

754

33

755   **Figure 5.** Summary of the timing of embryogenesis stages in *V. tsujii*. This represents the

756   complete range of first appearance of each features across multiple broods, including: yolk

757   separation (range = 5-8 days, N = 7); eye spot formation (range = 10-18 days, N = 12); upper lip

758   formation (range = 15-19 days, N = 3); limb formation (range = 18-23 days, N = 11); hatching

759   (range = 25-38 days, N = 11).

760

761   **Figure 6.** (A) K-means clusters of *Vargula tsujii* developmental stages based on carapace

762   height and width. Instar stages were assigned to each cluster via comparison to *P.*

763   *annecohenae* and additional analysis of male and female size dimorphism. (B) Points

764   representing laboratory cultured animals overlayed on wild caught and unknown data. Different

765   colors represent different clusters in the k-means analysis, and are labeled with their inferred

766   instar/adult stages. (C) Shows wild-caught animals dissected and identified as female in relation

767   to the k-means clusters, and (D) shows wild-caught animals dissected and identified as male in

768   relation to the k-means clusters.

769

770   **Figure 7.** Mitochondrial genome of V. tsujii. Note the duplicated control regions, CR1 and CR2

771   (in gray). Figure produced with Circos [78].

772

773

774

775

776

777

778

779

780

781 **Tables**

782 **Table 1.** Species of bioluminescent metazoans for which cultures are known to exist, including

783 information on the luciferin used for luminescence, estimated generation times, and whether the

784 luciferin used is synthesized via the genome of the luminescent organism itself (autogenic).

Species	Phylum	Luciferin	Autogenic luciferin?	Generation time	Citations
Mnemiopsis leidyi, Bolinopsis infundibulum, Leucothea pulchra	Ctenophora	coelenterazine	Possibly	~13 days (based on *M. mccradyi*)	80–83
Clytia haemispherica	Cnidaria	coelenterazine	No	~14 days (based on other *Clytia*)	65,84
Amphiura filiformis	Echinodermata	coelenterazine	No	Unknown	85
Photuris spp. Aspisoma lineatum Aquatica lateralis Aquatica ficta	Arthropoda	beetle luciferin	Yes	3-24 months	17,69,70,86
Arachnocampa richardsae	Arthropoda	glow worm luciferin	Possibly	10-12 months	87–89
Pontodrilus litoralis	Annelida	earthworm luciferin	?	1-3 months	90
Oikopleura dioica	Chordata	?	?	5 days	91,92

785

786

787

788   **Table 2.** List of collections locations or attempted collection locations for *Vargula tsujii*.

789   Collection locations for which a latitude and longitude could not be determined were not figured,

790   but are included here.

Number	Location	Latitude	Longitude	Collected?
1	WMSC, Santa Catalina Island, CA, USA	33.445139	-118.4845	Yes
2	Shelter Island boat launch, San Diego, CA, USA	32.69	-117.2230288	Yes
3	Cabrillo Beach, San Pedro, CA, USA	33.7133066	-118.2836733	Yes
4	Goleta Beach Pier, Goleta, CA, USA	34.4140665	-119.8287077	Yes
5	Santa Catalina Island, CA, USA	33.375	-118.6105556	Yes [33]
6	Un-named site	33.3805556	-117.5819444	Yes [33]
7	Un-named site	33.5797222	-118.1380556	Yes [33]
8	Santa Monica Pier, Santa Monica, CA, USA	34.0008333	-118.5777778	Yes [33]
9	Pinos Point, Pacific Grove, CA, USA	36.6658333	-121.9583333	Yes [33]
10	Seaport Village Pier, San Diego, CA, USA	32.708943	-117.171855	No

11	Shelter Island Police Dock, San Diego, CA, USA	32.709057	-117.235108	No
12	Mission Point, San Diego, CA, USA	32.761427	-117.245091	No
13	Mission Bay - Pacific Passage, San Diego, CA, USA	32.773906	-117.2103887	No
14	Dana Point Harbor, Dana Point, CA, USA	33.460975	-117.6991366	No
15	Balboa Peninsula Point, Newport Beach, CA, USA	33.599048	-117.884112	No
16	Balboa Beach Pier, Newport Beach, CA, USA	33.6075	-117.9288	No
17	Los Alamitos Bay, Long Beach, CA, USA	33.7524344	-118.1138442	No
18	Redondo Beach, CA, USA	33.84519	-118.3957644	No
19	Marina del Rey, CA, USA	33.9762886	-118.4456442	No
20	Santa Monica Pier, Santa Monica, CA, USA	34.0093	-118.4967	No
21	Prisoners Harbor, Channel Islands National Park, CA, USA	34.020384	-119.684361	No
22	Ventura Harbor boat ramp, Ventura, CA, USA	34.249224	-119.2632388	No

23	Ventura Harbor Pier, Ventura, CA, USA	34.273498	-119.291992	No
24	Santa Barbara Harbor, Santa Barbara, CA, USA	34.406417	-119.690501	No
25	Santa Barbara Harbor boat ramp, Santa Barbara, CA, USA	34.408094	-119.692132	No
26	Stearns Wharf, Santa Barbara, CA, USA	34.411296	-119.687706	No
27	Monterey Bay Pier, Monterey, CA, USA	36.6050389	-121.8919972	No
28	Monterey Bay Aquarium, Monterey CA, USA	36.6186583	-1219014222	No
29	Half Moon Bay, CA, USA	37.501913	-122.482173	No
30	Bodega Harbor, Bodega Bay, CA, USA	38.3333806	-123.0497833	No
-	La Jolla, CA, USA	unknown	unknown	Yes [33]
-	Bahia Los Angeles, Baja California, Mexico	unknown	unknown	Yes [33]

791

792

793

794

795

796

797   **Table 3.** Measurements for each cluster (and inferred instar) of *Vargula tsujii* ± SD.

Instar	N	Carapace Length (mm) ± SD	Carapace Height (mm) ± SD	Eye width (mm) ± SD
Embryo	84	0.418 +- 0.0271	0.326 + 0.0112	0.0630 + 0.0112
A-V	106	0.687 +- 0.0504	0.427 + 0.0289	0.0682 + 0.0164
A-IV	89	0.863 +- 0.0448	0.517 + 0.0374	0.0684 + 0.0271
A-III	66	1.078 +- 0.0516	0.632 + 0.0494	0.121 + 0.0208
A-II	96	1.214 +- 0.0426	0.711 + 0.0409	0.133 + 0.0160
Male A-1/Female A-1/ Adult Male	106	1.581 +- 0.0605	0.913 + 0.0402	0.226 + 0.0345
Adult Female?	70	1.983 +- 0.0798	1.154 + 0.0591	0.210 + 0.0326

798

799

800

801

802

803

804

805

806

807

808

809

810   **Table 4**: Comparison of embryogenesis timing between five different ostracod species post-

811   deposition. Species with an asterisk (*) are bioluminescent cypridinids.

Species	Cloudy Embryo	Yolk Sep.	Eye Spot Formation	Upper Lip	Limbs	Release	Citation
Vargula annecohenae *	2-3 days	9 days	14-15 days	17 days	-	19 days	[27]
Euphilomedes carcharodonta	-	14 days	58-70 days	-	14-41 days	65-75 days	[30]
Vargula hilgendorfii *	-	1-2 Days	6-8 days	6-8 days	4-5 days	16 days	[28]
Vargula tsujii *	3-4 days	5-8 days	10-18 days	15-19 days	18-23 days	25-38 days	This study
Xestoleberis hanaii	-	-	-	-	-	9-11 days	[32]

812

813

814

815

816

817

818

819

820

821

822

823

824

825

826

827   **Supplementary Materials**

828   **Table S1.** List of specimens examined in this paper for which sequences were obtained,

829   including locality, museum collection numbers (where applicable), and GenBank accession

830   numbers for the two genes sequenced (COI and 16S).

831

832   **Table S2.** Raw measurements of *Vargula tsujii* individuals, including carapace height and

833   length, keel width and eye width.

834

835   **Table S3.** Unfiltered library sequencing statistics for *V. tsujii*.

836

837   **Figure S1.** Traversal of the cleaned SPAdes *V. tsujii* mitochondrial genome assembly graph

838   nodes plotted by Bandage (gray). The single circularizing path representing the collapsed

839   duplicate control regions are shown in blue. The black stroke shows the path traversed through

840   the assembly graph followed to produce the circularized mtDNA FASTA file with two control

841   region, matching the structure of the V. hilgendorfii mtDNA (Ogoh and Ohmiya 2004).

842

843   **Figure S2.** Results for our 16S DAPC model test to determine the number of clusters that is

844   favored via comparison of Bayesian Information Criterion (BIC) values.

845

846   **Figure S3.** Results for our COI DAPC model test to determine the number of clusters that is

847   favored via comparison of Bayesian Information Criterion (BIC) values.

848

849   **Figure S4.** Cluster membership based on our 16S DAPC analysis compared with the original

850   population designation for each specimen. Overall, the clusters are not representative of any

851   population-level structure.

852

853   **Figure S5.** Cluster membership based on our 16S DAPC analysis compared with the original

854   population designation for each specimen. Overall, the clusters are not representative of any

855   population-level structure.

856

857   **Figure S6.** Exploded diagram of custom aquarium for rearing *Vargula tsujii*. A photo of built

858   aquarium is in main text, Figure 2. **A**. Plumbing components include 1. PVC pipe 1.5 inch

859   diameter. 2. PVC socket ball valve to control the rate of outflow 3. PVC 1.5 inch elbows 4. PVC

860   elbow with one side threaded to screw into 5. threaded bulkhead to span bottom of aquarium for

861   drainage 6. float switch valve to control water level (not shown on Figure 2 of main text). **B**.

862   Acrylic panels of ¼ inch thickness welded together with solvent include 7. Two panels of

863   dimension 16.5 x 13.25 inches that form the long sides of the aquarium 8. Two panels of

864   dimension 8 x 10.75 inches that form the short sides of the aquarium. One of these panels has

865   a hole drilled for the water inflow and float switch 9. One panel of 16.5 x 7.5 inches to form the

866   bottom of the aquarium, including a hole drilled for the bulkhead 10. One panel of 16.5 x 7.5

867   inches to forms a false bottom for the aquarium similar to the bottom of an undergravel

868   aquarium filter. We drilled small holes throughout to allow water but not sand to flow through.

869   (Not shown on Figure 2). In practice, we welded legs on the false bottom to allow it to stand on

870   the true bottom of the aquarium above the height of the bulkhead drain.